GEOPHYSICS, VOL. 52, NO. 7 (JULY 1987); P. 943–964, 20 FIGS.

A new slant on seismic imaging: Migration and integral geometry

In contrast, the classical diffraction stack always provides a ... tial from its projections, i.e., from seismic data. The problem of

are surfaces in model space that come from fixing a point $\mathbf{d} = (\mathbf{r}, \mathbf{s}, t)$ in the data and finding the surface of image points

sponding pair of projection operators (Miller, 1983):

medium, so that

$$\nabla^2 G_0(\mathbf{x}, \mathbf{y}, \omega) + \frac{\omega^2}{c_0^2(\mathbf{x})} G_0(\mathbf{x}, \mathbf{y}, \omega) = -\delta(\mathbf{x} - \mathbf{y}). \quad (6)$$

With these definitions, equation (4) can be recast as an integral equation, analogous to the Lippman-Schwinger equation of quantum mechanics (see, e.g., Taylor, 1972),

$$u(\mathbf{y}, \mathbf{s}, \omega) = G_0(\mathbf{y}, \mathbf{s}, \omega) + \omega^2 \int d^3\mathbf{x}\; G_0(\mathbf{y}, \mathbf{x}, \omega) f(\mathbf{x}) u(\mathbf{x}, \mathbf{s}, \omega).$$

When evaluated at receiver position $\mathbf{r}$, this equation gives the observed total field as a sum of the incident field within the background model G_0 plus the scattered field, represented by the integral term. Denoting the scattered field by

$$\left[\nabla_{\mathbf{x}}\, \tau(\mathbf{x}, \mathbf{y})\right]^2 = c_0^{-2}(\mathbf{x}), \quad (9)$$

and the amplitude or geometrical spreading term A satisfies the transport equation

$$A(\mathbf{x}, \mathbf{y}) \nabla_{\mathbf{x}}\, \tau(\mathbf{x}, \mathbf{y}) 2 \nabla_{\mathbf{x}} A(\mathbf{x}, \mathbf{y}) \cdot \nabla_{\mathbf{x}'}(\mathbf{x}, \mathbf{y}) = 0, \quad (10)$$

along the ray connecting the points $\mathbf{x}$ and $\mathbf{y}$.

Substituting for G_0 in equation (8) gives

$$u_{sc}(\mathbf{r}, \mathbf{s}, \omega) = \omega^2 \int d^3\mathbf{x}\; A(\mathbf{r}, \mathbf{x}) A(\mathbf{x}, \mathbf{s}) \times \exp\left\{ i\omega \left[\tau(\mathbf{r}, \mathbf{x}) + \tau(\mathbf{x}, \mathbf{s}) \right] \right\} f(\mathbf{x})$$

$$= \omega^2 \int d^3\mathbf{x}\; A(\mathbf{r}, \mathbf{x}, \mathbf{s}) \exp\left[i\omega\tau(\mathbf{r}, \mathbf{x}, \mathbf{s}) \right] f(\mathbf{x}). \quad (11)$$

will contain a convolution with the source wavelet. One can then shift the time derivative onto the source wavelet itself (see Tarantola, 1984). For reasons explained in a later section, we keep these equations in the given form. In the final section, we briefly discuss the effect of a band limited source.

Analogy with the classical Radon transform

As **r**, **s**, and t vary over the data, the acoustic GRT gives weighted integrals of the scattering potential over isochron surfaces in the model. We derive an approximate inverse formula (Radon, 1917; Gel'fand et al., 1966; Deans, 1983)

$$f(\mathbf{x}_0) = -\frac{1}{8\pi^2}\int d^2\xi\left[\frac{\partial^2}{\partial p^2}\, f^{\Delta}(\xi, p)\right]_{p=\xi\cdot\mathbf{x}_0}$$
$$= -\frac{1}{8\pi^2}\int d^2\xi\, \frac{\partial^2}{\partial p^2}\, f^{\Delta}(\xi, p = \xi\cdot\mathbf{x}_0). \qquad (16)$$

Equation (16) is the 3-D version of the filtered backprojection algorithm of X-ray tomography (see, e.g., Herman, 1980). For fixed ξ, the function $f^{\Delta}(\xi, p)$ is a one-dimensional function of p

equation (15), we can write for the filtered transform

$$\frac{\partial^2}{\partial p^2}\, f^{\Delta}(\xi, p) = \frac{\partial^2}{\partial p^2}\int d^3\mathbf{x}\ \delta(p - \xi\cdot\mathbf{x})f(\mathbf{x})$$
$$= \int d^3\mathbf{x}\ \delta''(p - \xi\cdot\mathbf{x})\,f(\mathbf{x}).$$

Combining this with equation (16) gives

$$f(\mathbf{x}_0) = -\frac{1}{8\pi^2}\int d^2\xi \int d^3\mathbf{x}\ \delta''\left[\xi\cdot(\mathbf{x}_0 - \mathbf{x})\right]f(\mathbf{x}). \qquad (17)$$

ing gives directly what may be called a "filtered" generalized

Radon transform. To obtain the identification, first shift the

Consider first $\nabla_{\mathbf{x}}\, \tau(\mathbf{r}, \mathbf{x}_0)$. Since rays are perpendicular to surfaces of equal traveltime (phase) and traveltime increases as $\mathbf{x}_0$ moves away from $\mathbf{r}$, this gradient points in the opposite direction from the ray that leaves $\mathbf{x}_0$ and reaches $\mathbf{r}$ in the background model, or along the ray that arrives at $\mathbf{x}_0$ from $\mathbf{r}$.

arrives at $\mathbf{x}_0$ from the source $\mathbf{s}$. The geometry is illustrated in Figure 6. We call these gradient vectors the incident and scattered rays at the image point $\mathbf{x}_0$.

From the eikonal equation (9), the magnitudes of the incident and scattered rays are equal to $1/c_0(\mathbf{x}_0)$, the slowness of the background model at the point $\mathbf{x}_0$. The total traveltime

gives the weighting function dW directly,

$$dW(\mathbf{r}, \mathbf{x}_0, \mathbf{s}) = \frac{1}{\pi^2} d^2\xi(\mathbf{r}, \mathbf{x}_0, \mathbf{s}) \frac{|\cos^3 \alpha(\mathbf{r}, \mathbf{x}_0, \mathbf{s})|}{c_0^3(\mathbf{x}_0) A(\mathbf{r}, \mathbf{x}_0, \mathbf{s})}, \quad (26)$$

and the final inversion formula

$$\langle f(\mathbf{x}_0) \rangle = \frac{1}{\pi^2} \int d^2\xi(\mathbf{r}, \mathbf{x}_0, \mathbf{s}) \times \frac{|\cos^3 \alpha(\mathbf{r}, \mathbf{x}_0, \mathbf{s})|}{c_0^3(\mathbf{x}_0) A(\mathbf{r}, \mathbf{x}_0, \mathbf{s})} u_{sc}(\mathbf{r}, \mathbf{s}, t = \tau_0). \quad (27)$$

The inversion integral we have derived is given explicitly in

The analysis described above carries through with only minor changes to yield the 2-D acoustic inversion formula

$$\langle f(\mathbf{x}_0)\rangle = \frac{1}{\pi}\int d\xi(\mathbf{r}, \mathbf{x}_0, \mathbf{s})$$

er here zero-offset and fixed-offset experiments in a constant background velocity. The zero-offset migration formula was first derived in Norton and Linzer (1981) by a different approach; the fixed-offset formula was derived in Beylkin (1985).

Zero-offset migration

factor $A(\mathbf{r}, \mathbf{x}, \mathbf{r}) = (4\pi|\mathbf{x} - \mathbf{r}|)^{-2}$ and substituting into equation (27) yields

$$\langle f(\mathbf{x})\rangle = \frac{16}{c_0^3}\int_{r_3=0} d^2\mathbf{r}\,\frac{x_3}{|\mathbf{x}-\mathbf{r}|}\,u_{sc}(\mathbf{r}, t = 2|\mathbf{x}-\mathbf{r}|/c_0)$$
$$= \frac{16}{c_0^3}\int d^2\mathbf{r}\cos\theta\,u_{sc}(\mathbf{r}, t = 2|\mathbf{x}-\mathbf{r}|/c_0). \quad (29)$$

A second algebraic derivation follows directly from equation (28). By definition, the surface integral

where the magnitude of the vector cross-product is the Jacobian factor. This again yields equation (29); moreover, if the data are collected on an irregular surface $r_3 = r_3(r_1, r_2)$, the only change in the derivation is that the third component of ξ becomes $x_3 - r_3(r_1, r_2)$. The latter construction works whenever it is possible to specify ξ explicitly in terms of the Cartesian coordinates of the experiment.

Fixed-offset experiments

Consider next a fixed-offset experiment on the surface of a half-space with constant background velocity. The experiment

source-receiver pair. Let $\mathbf{h} = (h_1, h_2, 0)$ be the half-offset vector, so that the receiver position $\mathbf{r} = \mathbf{m} + \mathbf{h}$ and the source

$$\xi = \frac{}{\left[2 + (\mathbf{x}-\mathbf{s})\cdot(\mathbf{x}-\mathbf{r})/|\mathbf{x}-\mathbf{s}|\,|\mathbf{x}-\mathbf{s}|\right]^{1/2}}$$
$$\times\left(\frac{\mathbf{x}-\mathbf{r}}{|\mathbf{x}-\mathbf{r}|} + \frac{\mathbf{x}-\mathbf{s}}{|\mathbf{x}-\mathbf{s}|}\right). \quad (31)$$

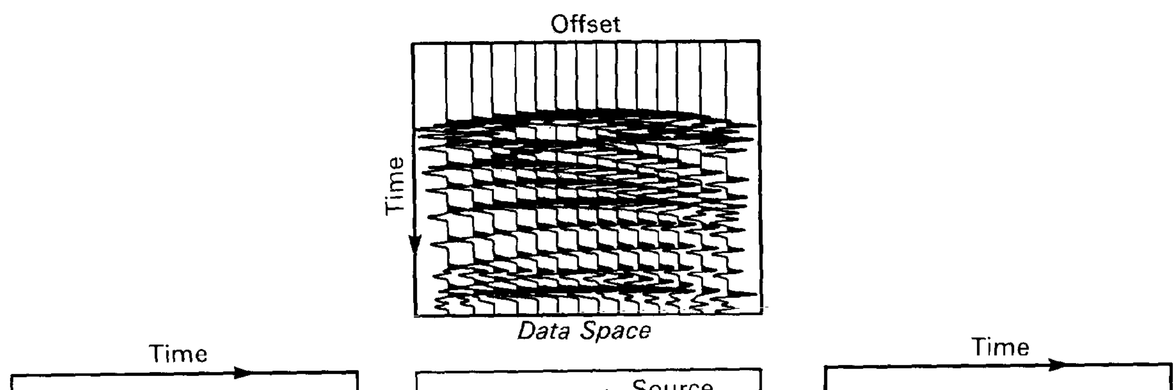

(a)

(b)


(m)
-200.0 -150.0 -100.0 -50.0 0.0 50.0 100.0 150.0
00.0
(m)
-200.0 -150.0 -100.0 -50.0 0.0 50.0 100.0 150.0
00.0

A change of variables can now be made from ξ to $\mathbf{m}$ using equations (30) and (31); however, the algebra is dense. For simplicity, consider the 2-D case and work with the angular variables defined in Figure 7; the polar angle θ determines ξ

source to the image point $\mathbf{x}$, and α_r is the angle between the vertical and the ray from the receiver to the image point $\mathbf{x}$. Then,

$$\theta = \frac{1}{2}(\alpha_s + \alpha_r) + \pi$$

$$= \frac{1}{2}\left(\tan^{-1}\frac{m-h}{z} + \tan^{-1}\frac{m+h}{z}\right) + \pi, \qquad (32)$$

in the scattering potential. Consider the velocity function defined by the relation

$$c^{-2}(z) = 1 + \Theta(z - z_0),$$

depth of the reflector. Taking $c_0^{-2} = 1$ gives the scattering potential

$$f(z) = \Theta(z - z_0).$$

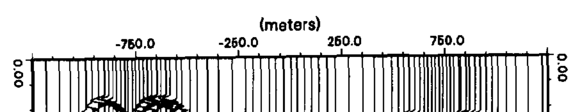

computed from integrals of f over hemispheres. It follows from coverage of tangent planes passing through an image point;

faces, by setting the scattering potential to be

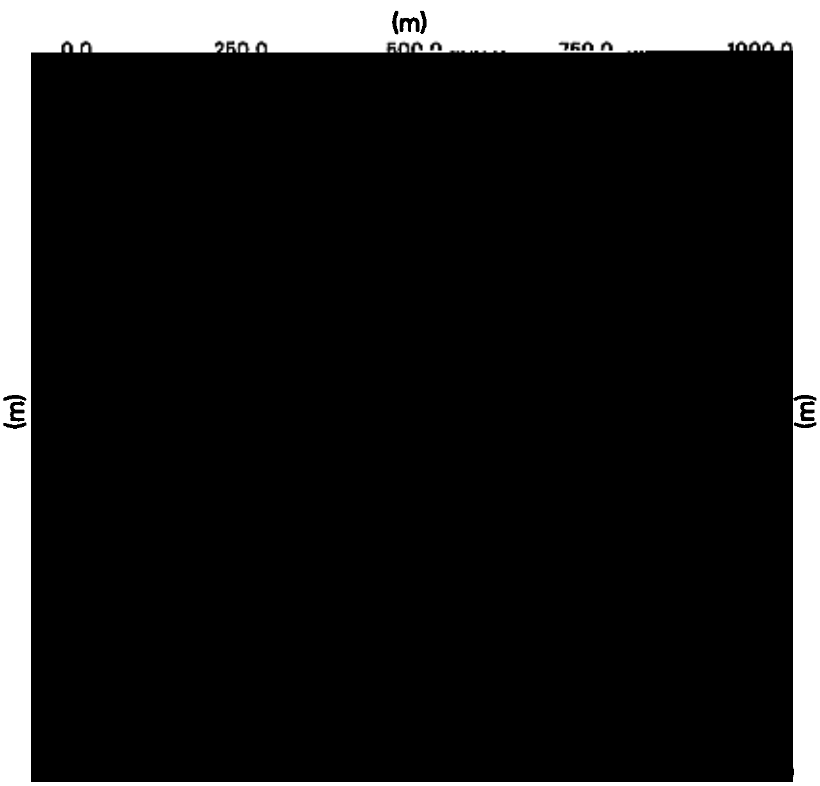

FIG. 15. Reconstruction from the synthetic DVSP experiment. (a) Ten wiggle plots showing profiles of the reconstruc-
[redacted]

[redacted]

multiple-receiver experiment with the source and receivers arranged as in Figure 1. The scattering object consisted of a family of point scatterers, which were separated by roughly one wavelength at the central frequency of the source and [redacted]

scattered data were obtained for 80 source-receiver pairs. The source wavelet was a Blackman-Harris window with a duration of 21.3 ms (which contains frequencies ranging from 0 to about 50 Hz).

[redacted]

mining the shapes and locations of the surfaces, the method is easily adapted to general source-receiver geometries and velocity models. Moreover, the dependence of spatial resolution on the geometry of the experiment, the reconstruction algorithm, and the assumptions about the medium is explicit in [illegible]

[illegible] performing just surface experiments, just borehole experiments, or both. It is also possible to describe an ideal experiment for a given configuration. [illegible]

perimental geometry and the finite bandwidth of the source wavelet.

The first issue is the relation between the available source-receiver pairs and the spatial dip spectrum of the reconstructed object. Locally, a restriction on the number of source [illegible]

[illegible] surfaces in the generalized Radon transform, and hence, the set of tangent planes (parameterized by ξ) available at each image point. Recall from the discussion of the classical Radon [illegible]

[redacted]

$$\Delta p = \frac{c_0(\mathbf{x}_0)}{2\cos\alpha}\,\Delta t. \qquad (36)$$

surface. This last figure illustrates the obliquity effect directly in the image domain.

The mapping of the data into the spatial Fourier spectrum


(sec.)
0.25
0.30
0.35
(m)
-75.0
-50.0
-25.0
0.0
25.0
50.0
75.0

borehole seismic profiles: A case study: Presented at the 55th Ann. Internat. Mtg., Soc. Explor. Geophys., Washington, D. C.,; abstracts and biographies 105–107.

Miller, D. E., 1983, Integral transforms and the migration of multiple-offset borehole seismic profiles: Research Note, Schlumberger-Doll Research.

Miller, D. E., and Dupal, L., 1986, Reef delineation by multiple offset

by its Fourier integral yielding

integrals which express these derivatives exist. For large ω